SHOCK TUBE SPECTROSCOPY LABORATORY

THE PHOTOSPHERIC ABUNDANCE OF IRON

*

George L. Withbroe

HARVARD COLLEGE OBSERVATORY

60 GARDEN STREET

CAMBRIDGE, MASS

THE PHOTOSPHERIC ABUNDANCE OF IRON

*

George L. Withbroe

Scientific Report No. 30

Harvard College Observatory

August 1968

ABSTRACT

The center-to-limb variation of equivalent widths of 198 Fe I lines in the spectral region 5500 to 7000 Å was studied with five photospheric models. The gf-values of Corliss and Warner were used in the analysis. The photospheric iron abundance was found to vary with excitation potential. This can be explained by a systematic error in the gf-values of high excitation lines and an error of 250 to 500 °K in the temperature of the arcs used for measuring the gf-values. Departures from LTE in the solar Fe I lines are also a possibility. The adopted photospheric abundance of iron, $\log \left(N_{Fe}/N_H\right)$ is -5.41.

I. INTRODUCTION

It is well known that there is evidence for a systematic difference between the coronal and photospheric abundances of iron (Müller 1966). The coronal abundance appears to be larger than the photospheric abundance by a factor of 10 to 20. This may represent a real difference in composition of the two regions or, alternatively, it may be that the compositions are the same and that the abundance determinations are affected by invalid assumptions or systematic errors. In this paper we consider problems connected with photospheric determinations, and describe results of an analysis of the center-to-limb variations of the equivalent widths for lines of neutral iron.

Müller and Mutschlecner (1964) made a similar study for a number of elements in the iron group. They found that the abundances of these elements did not vary significantly with either excitation potential or with position on the solar disk. They concluded that the assumption of local thermodynamic equilibrium (LTE) appears to be an adequate approximation for the lines studied. In their study Müller and Mutschlecner were handicapped by the lack of oscillator strengths for weak iron lines and therefore were able to use only moderately strong lines. Soon after their work was completed the extensive tables of gf-values compiled by Corliss and Warner (1964) became available. These tables contain oscillator strengths for many iron lines which are weak in the solar spectrum. Goldberg, Kopp, and Dupree (1964) and Aller, O'Mara, and Little (1964) used these gf-values and spectra from the center of the solar disk to determine iron abundances. Neither group found significant variations of the iron abundance with excitation potential. However, Dupree (1968) has re-examined the data of Goldberg, Kopp, and Dupree and has found some evidence for a dependence upon wavelength and excitation potential. Warner (1964) first discovered a variation of the solar iron abundance with excitation potential, which he and Cowley (Cowley and Warner 1967a, 1967b) later attributed to errors in Corliss and Warner's gf-values for high excitation lines. The purpose of the present paper is to investigate more completely the dependence of the photospheric iron abundance upon limb position, excitation potential, and the model photosphere used in the analysis.

II. OBSERVATIONS

The observations, which are the same as those used by Müller and Mutschlecner, are photoelectric tracings made at the McMath-Hulbert Observatory. We selected 172 Fe I lines in the spectral region 5500 to 7000 Å for study. They were chosen so that they would be free from blending by neighboring spectral lines. Equivalent widths were measured at three limb positions, cos θ = 1.0, 0.5, and 0.3, where θ is the angle between the line-of-sight and the outward normal to the solar surface. Table 1 contains a list of the measured equivalent widths. Twenty-six Fe I lines measured by Müller and Mutschlecner were also used in our study.

III. THEORY

In the calculation of theoretical equivalent widths the method of weighting functions was used. The line depth, r, was computed by a procedure very similar to that used by Aller, Elste, and Jugaku (1957). The line depth is given by the equation

$$r(\Delta\lambda) = \frac{I_\lambda - I_\ell(\Delta\lambda)}{I_\lambda} = \int_0^\infty \frac{\kappa_\ell(\Delta\lambda)}{\kappa_\lambda} \exp\left[- \int_0^{\tau_\lambda} \frac{\kappa_\ell}{\kappa_\lambda}(\Delta\lambda)\frac{dt}{\mu}\right] g_\lambda(\tau_\lambda)\frac{d\tau_\lambda}{\mu}$$

where I_λ is the emergent intensity in the continuum, $I_\ell(\Delta\lambda)$ is the emergent intensity in the line at a distance $\Delta\lambda$ from the center of the line, κ_λ is the continuous absorption coefficient per hydrogen particle, $\mu = \cos\theta$, and $g_\lambda(\tau_\lambda)$ is the weighting function (e.g. Aller 1960). The line absorption coefficient, κ_ℓ, is proportional to $(N_{Fe}/N_H) \cdot (N_\ell/N_{Fe})$ where N_{Fe}/N_H is the solar abundance of iron with respect to hydrogen, and N_ℓ is the number of atoms per cm^3 in the lower level of the transition producing the line. The quantity N_ℓ/N_{Fe} may be expressed as a function of the photospheric electron temperature and density by using Boltzmann's and Saha's equations. Unless otherwise stated, LTE was assumed.

The equivalent widths were evaluated from the formula

$$W_\lambda = \int_{-\infty}^{\infty} r(\Delta\lambda)\, d(\Delta\lambda).$$

The equivalent width of a weak line can be related to the solar abundance, N_{Fe}/N_H, by an equation of the form

$$\log W_\lambda/\lambda = \log N_{Fe}/N_H + \log gf\lambda - \theta_\circ\, \chi_\ell + \log C_\lambda,$$

where g is the statistical weight of the lower level of the transition; f is the oscillator strength of the line;

λ is the wavelength; χ_{ℓ} (ev) is the excitation potential of the lower level of transition; and C_{λ} depends upon the photospheric model, κ_{λ}, and the ionization properties of iron. The quantity $\theta_{\circ} = 5040/T_{\circ}$ may be taken as unity for the sun, $T_{\circ}$ representing a mean temperature in the atmospheric layers where the lines are formed.

An empirical curve-of-growth is obtained by plotting observed values of log W_{λ}/λ as a function of

$$\log gf\lambda - \theta_{\circ}\,\chi_{\ell} + \log C_{\lambda}.$$

By comparing theoretical and empirical curves-of-growth one can obtain a value for log (N_{Fe}/N_{H}). A mean curve-of-growth for all of the lines at $\mu = 1.0$ is shown in Figure 1.

IV. PHOTOSPHERIC MODELS

In interpreting the observations we used five recent photospheric models. The first of these, Mutschlecner's (1963), is the one used by Müller and Mutschlecner (1964) in their analysis of the center-to-limb behavior of lines of the iron group of elements. The second model, Elste's (1967) Model 10 was derived from an analysis of limb-darkening observations of the spectral continuum. This model, and its slightly different predecessor Model 9, have been used to explain the center-to-limb variation of the wings of the Na D lines (Mattig and Schröter 1961, Mugglestone 1964), the variation of the wings of the hydrogen Balmer lines (David 1961), and the center-to-limb variation of profiles and equivalent widths of CH lines (Withbroe 1967a). The third model, Holweger's (1967), was derived from an analysis of limb-darkening observations of the spectral continuum and an analysis of the center-to-limb variation of the equivalent widths and central intensities of a number of spectral lines. This model was constructed by assuming LTE consistently throughout the photosphere and lower chromosphere. The fourth model, the Utrecht Reference Model (Heintze, Hubenet, and Jager 1964), differs from the first three in that it contains a temperature minimum located at a fairly large optical depth, $\tau_{5000} = 0.02$. The last model is a preliminary inhomogeneous three-steam model developed by Elste (1967) from Model 10 and Edmonds' (1962) measurements of the center-to-limb behavior of the photospheric granular contrast. The variation of temperature with optical depth of the different models is given in Figure 2.

V. RESULTS

Table 2 summarizes the abundances calculated with Mutschlecner's photospheric model and an isotropic depth-independent microturbulence with a magnitude of 1.8 km/sec. The first column gives the mean excitation potential used in constructing the theoretical and empirical curves-of-growth. The other columns give iron abundances, log (N_{Fe}/N_H), for different positions on the solar disk and the number of lines used. Note that the abundance changes very little with limb position. This is in essential agreement with the results of Müller and Mutschlecner (1964). The abundances at $\mu = 0.5$ and at $\mu = 0.3$ are slightly larger than the abundance at $\mu = 1.0$; however, as will be shown below, these differences can be eliminated by choosing a different photospheric model and/or microturbulence model.

There is another more disturbing trend: the abundance seems to vary with the lower excitation potential, χ_ℓ. This is shown more clearly in Figure 3. The abundance decreases with increasing χ_ℓ, reaches a minimum at about 4 volts, and then increases again. The behavior at all three limb positions is the same. Warner (1964) found a similar effect, using a less sophisticated photospheric model, the Milne-Eddington model, and observations made at the center of the solar disk. He suggested that the sharp change in slope at $\chi_{\ell} \approx 4$ volts might be caused by (1) incorrect gf-values for lines with $\chi_{\ell} > 4$ volts, (2) a non-LTE overpopulation of energy levels for large depths, or (3) peculiarities in the mechanism of line formation. Jefferies (1966) suggested that the effect was caused by a non-LTE underpopulation of energy levels of low excitation lines and that this can be used to explain the difference between the photospheric and coronal abundances of iron. More recently Cowley and Warner (1967a, b) and Withbroe (1967b) independently concluded that the first of Warner's explanations is the correct one, and that the source of difficulty is a calibration error for gf-values included in Corliss and Warner's (1964) tables.

The great majority of the gf-values for lines of interest in the present investigation are based upon measurements made by Corliss and Bozman (1962) and Corliss and Warner (1964) hereafter called CB and CW respectively. These gf-values were placed on an absolute scale by applying a calibration function that is independent of χ_u for $2.1 \le \chi_u \le 6.0$ volts and varies with χ_u outside this range. The quantity χ_u is the excitation potential of the upper level of the transition producing the spectral line. A value of $\chi_u = 6.0$ volts corresponds closely to $\chi_\ell = 4.0$ volts for lines with wavelengths between 5500 Å and 7000 Å. The reasons for introducing χ_u-dependent correction for $\chi_u > 6.0$ volts are documented by Corliss and Bozman (1962).

Huber and Tobey (1967, 1968) and Warner and Cowley (1967) found indications that this calibration function is incorrect. Huber and Tobey measured Fe I gf-values between 3000 and 4000 Å and found a systematic variation between their gf-values and Corliss and Warner's that depends upon χ_u in almost exactly the same manner as the CB calibration function. Their results suggest that the χ_u-dependent correction applied to the CW gf-values for $\chi_u > 6.0$ volts should be removed. Warner and Cowley came to the same conclusion by analysing Ti II gf-values and constructing a model for the CB arc. Corliss and Tech (1967) have very recently published a revised list of Fe I gf-values which incorporates these results. These values were not available at the time of the present study, but are essentially equal to the corrected values described below.

If the CW gf-values are corrected by removing the dependence upon χ_u from the CB calibration function, the result shown in Figure 4 is obtained. Now the photospheric abundance shows a significant decrease with increasing excitation potential. The slopes of the lines drawn through the points are 0.09, 0.10, and 0.10 for $\mu = 1.0$, 0.5, and 0.3 respectively. This suggests that the excitation temperature of the solar Fe I lines is approximately 450 °K cooler than the photospheric electron temperature, about 5000 °K, in the region where the Fe I lines are formed.

The effect of modifying the CW gf-values is further illustrated in Figures 5 and 6. Iron abundances determined from individual Fe I lines for $\mu = 1.0$ are plotted as a function of χ_u in these figures. Only lines with $\log W_\lambda/\lambda < -4.8$ were used here, since abundances determined from individual lines are not very accurate for lines on the horizontal section of the curve-of-growth. For Figure 5 the published gf-values of Corliss and Warner (1964) are used. The light line drawn through the points is a linear curve whose parameters were determined by a least-squares analysis. The slope of the line is 0.007. The heavy line is a fourth degree curve. An examination of the points in this figure indicates why several investigators, who also used the CW gf-values, did not find a significant variation of log (N_{Fe}/N_H) with excitation potential. Goldberg, Kopp, and Dupree (1964) and Aller, O'Mara, and Little (1964) grouped together spectral lines with $\Delta\chi_\ell \geqslant 1$ volt in such a manner as to mask the dependence upon excitation potential visible in this figure. Warner (1964) first discovered an excitation potential dependence because he used smaller intervals, $\Delta\chi_\ell = 0.5$ volts.

Figure 6 shows how correcting the CW gf-values by removing the χ_u-dependence in the CB calibration function affects the abundances. A least squares analysis indicates that the data can be represented by a linear curve with a slope of -0.09 ± 0.01. Similarly, for $\mu = 0.5$ and $\mu = 0.3$ slopes of -0.10 ± 0.01 and -0.11 ± 0.01 are obtained. Similar calculations with Elste's Model 10 gives slopes of -0.09 ± 0.01, -0.10 ± 0.01, and -0.11 ± 0.01 for $\mu = 1.0$, 0.5, and 0.3 respectively.

Theoretical curves-of-growth were also calculated for the other photospheric models described in section III. The iron abundance was determined for 8 values of $\bar{\chi}_\ell$ using the corrected gf-values of Corliss and Warner. It was assumed that $\log (N_{Fe}/N_H) = A - \Delta\theta_e \cdot \bar{\chi}_\ell$ where $\Delta\theta_e = 5040/T_{ex} - 5040/T_\circ$, $T_\circ$ is the mean electron temperature in the region of line formation, and T_{ex} is the empirical excitation temperature of the Fe I lines. Values of the parameters A and $\Delta\theta_e$ were determined by application of the least squares technique. The abundance determined for each value of $\bar{\chi}_\ell$ was weighted by the number of lines contributing to the abundance determination. The resulting values of $\Delta\theta_e$ are given in Table 3. These values correspond to $\Delta T = T_\circ - T_{ex}$ of 250 to 500 °K.

This apparent difference between $T_\circ$ and T_{ex} could be caused by (1) inadequate photospheric models, (2) a departure from LTE, or (3) a χ-dependent error in the gf-values. It is doubtful whether the temperature difference can be attributed to inadequate solar models. The five chosen for this study are typical of recent models which have been used to explain a variety of center-to-limb observations of spectral continua and lines. A new model that would eliminate the difference between $T_\circ$ and T_{ex} would undoubtedly encounter severe difficulties in explaining the observations used in constructing the other models.

A more likely cause of the difference is a departure from LTE. A fundamental assumption used in deriving photospheric models has been the assumption of LTE.

There are a variety of opinions as to how well the population of the various atomic and molecular energy levels approach the values predicted under the assumption of LTE. Our results are evidence that the populations of the energy levels of Fe I are systematically different from the populations given by the Boltzmann equation and the use of the photospheric electron temperature. This difference can be characterized by specifying that the Fe I excitation temperature is 250 to 500 °K cooler than the photospheric electron temperature in the layers where the Fe I lines are formed, $\log \tau_{5000} \leq -0.5$.

It is significant that Holweger (1967) was able to construct a photospheric model which accounted for the limb darkening of the spectral continuum and the center-to-limb variation of the equivalent widths and central intensities of a number of spectral lines, including Fe I lines similar to those used in this investigation. The fact that we have found an excitation temperature for the Fe I lines that is markedly different, approximately 500 °K, from Holweger's temperatures suggests that our low excitation temperature may be caused by a systematic χ-dependent error in the gf-values of Corliss and Warner instead of a departure from LTE in the solar atmosphere.

As we have already indicated the gf-values used in this study are based primarily on measurements of Corliss and Bozman (1962) and of Corliss and Warner (1964). These measurements were made in free burning arcs which were assumed to be characterized by a single effective temperature and electron density. The validity of this assumption is questionable. For example, the model for the CB arc constructed by Warner and Cowley (1967), using Ti II observations, indicates that the CB arc may have consisted of a hot core surrounded by cooler outer layers. If the arc does contain significant inhomogeneities, the reliability of the mean temperature assigned to it will be affected. As an estimate of this reliability we will use the standard deviation of the temperature determinations made by Corliss and Bozman. In an analysis of 31 independent temperature determinations they found that the standard deviation of a single temperature measurement was 600 °K and that the standard deviation of the mean temperature was 110 °K. Since the temperature of Corliss and Warner's arc was determined with the CB gf-values, the standard deviation of the mean temperature of the CW arc must be equal to or greater than 110 °K. Furthermore, in view of the rather large error quoted for individual measurements of temperature, 600 °K, systematic errors of this magnitude cannot be ruled out. Such errors could produce a linear χ-dependence in the CB and CW gf-values. For example 110 °K and 600 °K errors correspond to χ-dependences of ± 0.02 and ± 0.12 dex per electron volt respectively. The results given in Table 3 suggest a χ-dependence of -0.08 dex per electron volt. Therefore, it appears possible that our results can be explained by an error in the temperature assigned to the CB arc.

This conclusion is further supported by a comparison of the CW gf-values with those of Byard (1967). Byard's gf-values are based upon measurements made in a shock tube. Huber (private communication) found that if values of $\Delta \log gf = \log gf(\text{Byard}) - \log gf_{CW}$ are plotted as a function of χ_u, $\Delta \log gf$ varies linearly with χ_u for lines with $\chi_u < 6.0$ volts. The slope of the line relating $\Delta \log gf$ to χ_u is -0.10. If the CW gf-values are corrected in the manner described earlier in this paper $\Delta \log gf$ varies linearly with χ_u over the range $2.4 \leq \chi_u \leq 6.8$ volts. The slope in this case also is -0.10. This is independent evidence that the CW gf-values may contain a χ-dependent error as large as 0.10 dex per electron volt and suggests that the χ-dependence in the photospheric abundance of iron is more likely to be caused by a systematic error in the gf-values than by a departure from LTE in the photosphere. Unfortunately, Byard (1967) by making an erroneous assumption on the extent of line broadening may have used too large a ratio of Lorentzian to Gaussian line width; thus the conclusion discussed here may be questioned.

Before concluding this section we should point out that the magnitude of the χ-dependence in the solar iron abundance depends critically upon the correction that is applied to the CW gf-values for lines with $\chi_u > 6.0$ volts. As we have already indicated, the results of Huber and Tobey (1967, 1968) and of Warner and Cowley (1967) indicate that this correction factor should be sufficiently large to cancel the effect of the χ-dependence in the calibration function used for defining the absolute scale of the CB and CW gf-values. However, their results do not completely rule out smaller correction factors which would reduce the magnitude of the χ-dependence found in the solar iron abundance. Additional independent laboratory measurements of gf-values for high excitation Fe I lines are needed to firmly establish the form of the correction factor.

VI. THE EFFECT OF DEPARTURES FROM LTE

In the previous section we presented evidence that the empirical Fe I excitation temperature is 250 to 500 °K cooler than the corresponding excitation temperature derived from several photospheric models. As we indicated, this may be caused by departures from LTE in the photosphere or by systematic errors in the gf-values, the second cause being the more probable of the two. However, suppose for the moment that there are departures from LTE of the indicated magnitude. What effect will they have on the determination of the photospheric iron abundance?

In an attempt to answer this question we calculated non-LTE curves-of-growth using Elste's Model 10, an excitation temperature varying with depth in the manner illustrated in Figure 7, and a non-LTE weighting function (Pecker 1959),

$$g_\lambda(\tau_\lambda) = \frac{\int_{\tau_\lambda}^{\infty} B[T_e(\tau)]\,e^{-\tau/\mu}\,d\tau/\mu - B[T_{ex}(\tau_\lambda)]\,e^{-\tau_\lambda/\mu}}{\int_0^{\infty} B(\tau)\,e^{-\tau/\mu}\,d\tau/\mu} ,$$

where B is the Planck function, T_e is the electron temperature, and T_{ex} is the excitation temperature. The depth-dependence of the excitation temperature was chosen so that the iron abundance would not vary significantly with χ_ℓ and also so that T_{ex} would become equal to the photospheric electron temperature at $\tau_{5000} \approx 1.0$. The ionization temperature was set equal to the electron temperature. The resulting iron abundances for $\mu = 1.0$, 0.5, and 0.3 are -5.22, -5.26, and -5.31 respectively. These values are systematically larger by an average of 0.15 dex than the corresponding values determined under the assumption of LTE with the same model. This suggests that the photospheric iron abundance is not appreciably affected by departures from LTE. Furthermore the effect is too small by an order of magnitude to explain the difference between the photospheric and coronal abundances of iron.

VII. THE PHOTOSPHERIC IRON ABUNDANCE

The iron abundances determined from all of the models used in the present analysis are summarized in Table 4. These abundances were determined by use of curves-of-growth calculated for the values of $\bar{\chi}_\ell$ listed in Table 2, and were obtained by averaging the abundance for each $\bar{\chi}_\ell$ weighted by the number of lines making up the empirical curve-of-growth. The gf-values used are those of Corliss and Warner, which were corrected by removing the

χ_u -dependence in the CB calibration function for $\chi_u > 6.0$ volts. If the abundances in Table 4 are averaged with equal weights we obtain

$$\log (N_{Fe}/N_H) = -5.41 .$$

If the χ-dependence in the abundance should prove to be an effect of non-LTE instead of an error in the gf-values, then the results of section V indicate that this value for $\log (N_{Fe}/N_H)$ should be increased to -5.26.

The adopted abundance, $\log (N_{Fe}/N_H) = -5.41$, is in good agreement with other recent determinations. Typical values are -5.41 (Aller, O'Mara and Little 1964); -5.36 (Goldberg, Kopp, and Dupree 1964); and -5.49 (Warner 1968).

VIII. SUMMARY

This work has established a number of points, (1) If the CW gf-values are used to determine the solar iron abundance, the resulting abundance varies with the excitation potential of the lines used. The variation of the abundance with χ_ℓ seems to reflect in part the influence of the correction factor applied to the CW gf-values for lines of high excitation. This confirms Warner's results, which were obtained with a less sophisticated photospheric model (2) If the CW gf-values are corrected in the manner suggested by Huber and Tobey (1967, 1968) and Warner and Cowley (1967), the iron abundance, log (N_{Fe}/N_H), appears to vary with χ_ℓ in a linear fashion. This may be interpreted as a departure from LTE of the order of 250 to 500 °K in the solar Fe I lines, or as a corresponding χ-dependent error in the corrected CW gf-values. (3) The determination of the solar iron abundance is not appreciably affected by the choice of photospheric model. (4) Departures from LTE in the excitation temperature of the solar Fe I lines have only a small effect on the abundance determination. (5) The best value of log (N_{Fe}/N_H) that results from this analysis is -5.41.

I would like to thank Dr. A.K. Dupree, Dr. L. Goldberg, and Dr. M.C.E. Huber for their helpful comments and suggestions. I would also like to thank Mr. Neal Baker for his assistance in measuring equivalent widths and computer programming.

This work was supported by the National Aeronautics and Space Administration through grant NsG-438 and contract NASw-184.

References

Aller, L.H. 1960, Stellar Atmospheres, ed. J.L. Greenstein (Chicago: University of Chicago Press); p.156.

Aller, L.H., Elste, G. and Jugaku, J. 1957, Ap. J. Suppl., **3**, 1.

Aller, L.H., O'Mara, B.J., and Little, S. 1964, Proc. Nat. Acad. Sci. Washington, **51** 1238.

Byard, P.L. 1967, J.Q.S.R.T., **7**, 559.

Cowley, C.R. and Warner, B. 1967a, Observatory, **87**, 117.

Cowley, C.R. and Warner, B. 1967b, A.J., **72**, 791.

Corliss, C.H. and Bozman, W.R. 1962, N.B.S. Monograph, No. 53.

Corliss, C.H. and Tech, J.L.,1967 NBS Monograph, No. 108.

Corliss, C.H. and Warner, B. 1964, Ap. J. Suppl. **8**, 395.

David, K.H. 1961, Zs. f. Ap., **53**, 37.

Dupree, A.K. 1968, Thesis, Harvard University.

Edmonds, F.N., Jr. 1962, Ap. J. Suppl. **6**, 357.

Elste, G.H.E. 1967, Ap. J., **148**, 857.

Goldberg, L., Kopp, R.A., and Dupree, A.K. 1964, Ap. J., **140**, 707.

Heintze, J.R.W., Hubenet, H., and Jager, C. de 1964, B.A.N., **17**, 442.

Holweger, H. 1967, Zs. f. Ap., **65**, 365.

Huber, M. and Tobey, F.L. , Jr. 1967, A.J. 72, 804

Huber, M. and Tobey, F.L., Jr. 1968, Ap. J., 152, 609.

Jefferies, J.T. 1966, Abundance Determination in Stellar Spectra , ed. H. Hubenet (London and New York: Academic Press), p. 207.

Mattig, W. and Schröter, E.H. 1961 , Zs. f. Ap., 52, 195.

Mugglestone, D. 1964, Colloquium, University of Michigan.

Müller, E.A. 1966, Abundance Determination in Stellar Spectra, ed. H. Hubenet,(London and New York: Academic Press) , p. 171.

Müller, E.A. and Mutschlecner, J.P. 1964, Ap. J. Suppl., 9, 1.

Mutschlecner J.P. 1963, thesis, University of Michigan .

Pecker, J.C. 1959, Ann. d'Ap., 22, 499.

Warner, B. 1964, M.N., 127, 413.

Warner, B. 1968, M.N., 138, 229.

Warner, B. and Cowley, C.R. 1967, J.Q.S.R.T., 7, 751.

Withbroe, G.L. 1967a, Ap. J., 147, 1117.

Withbroe, G.L. 1967b, A.J., 72, 837.

TABLE 1.

MEASURED EQUIVALENT WIDTHS OF FE I LINES (mÅ)

χ_{ℓ}	λ	$W_{\lambda}(\mu=1.0)$	$W_{\lambda}(\mu=0.5)$	$W_{\lambda}(\mu=0.3)$
.86	5956.706	54.3	60.1	66.6
.86	6358.687	88.6	89.9	93.9
.91	6400.323	71.0	69.7	77.8
.96	6498.945	43.7	56.2	56.5
.99	6574.254	24.1	29.6	33.7
1.01	6625.039	12.2	17.2	19.9
1.01	6648.121	4.9	8.2	9.2
1.48	6581.218	7.1	21.8	24.4
1.48	6710.323	12.3	17.5	22.2
2.18	6151.623	49.2	51.1	54.6
2.20	6137.002	64.2	65.1	72.0
2.20	6335.337	97.3	101.6	101.5
2.22	6082.718	31.5	37.9	41.8
2.22	6173.341	64.5	73.9	76.8
2.22	6213.437	80.6	87.0	83.8
2.22	6240.653	44.5	46.5	58.3
2.22	6297.799	74.8	83.7	78.4
2.28	6392.538	17.5	19.9	25.7
2.28	6421.360	98.2	118.9	113.2
2.28	6481.878	61.1	76.9	72.8
2.28	6608.044	14.4	18.6	20.6
2.40	6988.533	0.0	40.4	46.7
2.42	6663.448	77.6	78.9	83.4
2.42	6750.164	73.7	75.0	85.7
2.42	6861.945	14.5	24.6	22.6
2.43	6344.155	58.6	0.0	65.3
2.43	6393.612	137.2	137.5	134.3
2.43	6593.884	79.9	89.0	87.0
2.45	5916.257	53.7	64.5	58.0
2.45	6318.027	0.0	110.7	109.2
2.56	5701.557	83.2	83.9	85.8
2.56	6475.632	41.4	68.2	69.0
2.56	6609.118	64.3	62.1	73.0
2.56	6839.835	25.6	34.9	36.4
2.59	6005.551	20.5	22.6	26.9
2.59	6322.694	76.3	79.1	81.0
2.61	6200.327	71.7	73.1	79.1
2.73	6180.209	52.5	58.0	61.1
2.73	6806.856	30.3	35.3	39.0
2.76	6703.576	33.1	38.8	42.7

TABLE 1.

MEASURED EQUIVALENT WIDTHS OF FE I LINES (mÅ)

χ_ℓ	λ	$W_\lambda(\mu=1.0)$	$W_\lambda(\mu=0.5)$	$W_\lambda(\mu=0.3)$
.86	5956.706	54.3	60.1	66.6
.86	6358.687	88.6	89.9	93.9
.91	6400.323	71.0	69.7	77.8
.96	6498.945	43.7	56.2	56.5
.99	6574.254	24.1	29.6	33.7
1.01	6625.039	12.2	17.2	19.9
1.01	6648.121	4.9	8.2	9.2
1.48	6581.218	7.1	21.8	24.4
1.48	6710.323	12.3	17.5	22.2
2.18	6151.623	49.2	51.1	54.6
2.20	6137.002	64.2	65.1	72.0
2.20	6335.337	97.3	101.6	101.5
2.22	6082.718	31.5	37.9	41.8
2.22	6173.341	64.5	73.9	76.8
2.22	6213.437	80.6	87.0	83.8
2.22	6240.653	44.5	46.5	58.3
2.22	6297.799	74.8	83.7	78.4
2.28	6392.538	17.5	19.9	25.7
2.28	6421.360	98.2	118.9	113.2
2.28	6481.878	61.1	76.9	72.8
2.28	6608.044	14.4	18.6	20.6
2.40	6988.533	0.0	40.4	46.7
2.42	6663.448	77.6	78.9	83.4
2.42	6750.164	73.7	75.0	85.7
2.42	6861.945	14.5	24.6	22.6
2.43	6344.155	58.6	0.0	65.3
2.43	6393.612	137.2	137.5	134.3
2.43	6593.884	79.9	89.0	87.0
2.45	5916.257	53.7	64.5	58.0
2.45	6318.027	0.0	110.7	109.2
2.56	5701.557	83.2	83.9	85.8
2.56	6475.632	41.4	68.2	69.0
2.56	6609.118	64.3	62.1	73.0
2.56	6839.835	25.6	34.9	36.4
2.59	6005.551	20.5	22.6	26.9
2.59	6322.694	76.3	79.1	81.0
2.61	6200.327	71.7	73.1	79.1
2.73	6180.209	52.5	58.0	61.1
2.73	6806.856	30.3	35.3	39.0
2.76	6703.576	33.1	38.8	42.7

TABLE 1. CONTINUED.

χ_ℓ	λ	$W_\lambda(\mu=1.0)$	$W_\lambda(\mu=0.5)$	$W_\lambda(\mu=0.3)$
2.83	6311.504	24.7	31.1	32.8
2.83	6518.373	54.4	58.7	59.7
2.84	6229.232	35.0	40.8	42.7
2.84	6355.035	0.0	79.6	0.0
2.86	6270.231	53.4	54.5	59.2
3.33	6271.283	21.1	25.2	29.8
3.37	5586.771	216.2	0.0	0.0
3.40	5784.666	23.9	26.9	29.4
3.42	5712.138	52.9	52.5	54.9
3.60	6400.009	190.3	162.3	0.0
3.64	5539.293	14.8	20.4	23.3
3.64	5636.705	21.9	19.9	25.6
3.64	5760.359	20.9	24.9	25.5
3.64	5762.423	27.8	27.9	33.8
3.65	6232.648	85.0	88.4	86.0
3.68	6302.499	84.9	93.7	87.9
3.69	5543.199	62.6	61.0	60.7
3.69	6336.830	111.7	110.2	102.1
3.69	6408.026	110.0	100.7	98.6
3.88	5804.038	21.9	26.5	28.0
3.88	5809.224	49.3	50.6	54.0
3.88	6003.022	83.8	81.7	81.6
3.88	6008.566	88.2	85.4	86.8
3.88	6226.740	26.5	29.2	31.3
3.93	5798.195	40.8	43.6	46.5
3.93	5934.665	74.7	78.0	73.1
3.94	5976.787	0.0	71.3	73.4
3.94	6187.995	45.3	51.7	48.9
3.94	6411.658	147.5	136.5	131.1
3.98	5952.726	61.7	61.5	59.5
3.98	6096.671	33.0	39.5	40.6
4.07	6027.059	63.8	65.6	63.8
4.07	6157.733	59.8	65.4	63.6
4.07	6315.814	40.9	45.1	42.0
4.07	6639.897	13.5	15.9	17.5
4.07	6793.273	10.7	12.2	16.2
4.07	6857.251	19.0	23.1	26.9
4.10	6725.364	14.5	18.3	19.3
4.10	6999.885	0.0	57.1	55.4
4.14	5587.581	49.9	37.8	38.7

TABLE 1. CONTINUED

χ_ℓ	λ	W_λ (μ=1.0)	W_λ (μ=0.5)	W_λ (μ=0.3)
4.14	6127.912	46.8	50.0	51.6
4.14	6165.363	43.6	46.0	45.6
4.14	6240.318	13.1	17.7	18.3
4.14	6796.128	0.0	12.7	18.9
4.15	5620.497	36.3	33.6	33.5
4.15	6653.911	9.4	11.1	11.8
4.15	6916.686	0.0	54.4	65.5
4.18	5662.524	92.8	92.5	88.3
4.19	6215.149	65.5	74.8	77.4
4.19	6380.750	57.4	57.5	63.9
4.19	6436.413	8.5	11.1	12.0
4.19	6786.860	21.6	30.3	29.2
4.21	5522.454	45.0	0.0	44.8
4.21	5618.642	48.6	50.9	54.6
4.22	5538.522	37.4	38.6	43.0
4.22	5543.944	65.1	62.6	62.4
4.22	5638.271	0.0	77.5	76.0
4.22	5775.088	57.5	0.0	59.1
4.22	5793.922	33.3	34.3	0.0
4.23	5525.552	54.5	54.0	54.0
4.26	5635.831	37.3	34.5	38.6
4.26	5641.448	65.3	65.7	66.6
4.26	5652.327	24.9	26.6	28.2
4.26	5731.772	57.5	0.0	57.2
4.26	5741.856	29.8	32.9	33.2
4.26	5753.132	81.6	77.7	75.0
4.28	5661.355	20.4	23.8	25.2
4.28	5717.841	62.9	58.5	61.7
4.28	5814.815	21.4	24.3	27.2
4.29	5856.096	34.1	36.9	35.6
4.30	5705.473	40.4	0.0	40.9
4.37	5546.514	52.6	52.6	54.2
4.39	5619.608	33.5	35.7	35.0
4.39	5624.030	49.6	51.6	50.7
4.39	5653.874	40.4	39.8	37.4
4.43	5560.220	57.9	51.9	52.7
4.43	5562.716	60.8	61.3	60.7
4.43	5708.102	35.8	39.9	41.1
4.55	5554.900	101.2	79.5	68.7
4.55	5686.540	73.7	0.0	67.3

TABLE 1. CONTINUED

χ_{ℓ}	λ	$W_{\lambda}(\mu=1.0)$	$W_{\lambda}(\mu=0.5)$	$W_{\lambda}(\mu=0.3)$
4.55	5752.042	58.2	55.0	56.0
4.55	5852.228	39.8	41.9	40.1
4.55	5859.596	78.6	74.4	79.7
4.55	5862.368	88.7	84.1	87.9
4.55	5929.682	39.2	39.9	39.5
4.55	5983.688	63.7	67.2	65.1
4.55	6024.068	115.6	107.2	103.2
4.55	6627.560	24.3	25.6	30.9
4.55	6843.655	58.8	62.1	61.0
4.56	6633.758	63.6	67.3	64.3
4.56	6737.978	19.7	19.4	21.8
4.56	6855.166	72.6	79.2	70.2
4.56	6862.496	27.1	31.8	32.5
4.58	6364.706	12.8	13.4	15.4
4.58	6667.740	9.3	10.4	12.4
4.58	6716.252	16.3	16.2	19.0
4.58	6804.297	12.4	18.6	16.2
4.59	6591.326	8.9	13.0	11.7
4.59	6837.013	14.3	19.8	20.4
4.61	5806.732	55.8	54.3	54.1
4.61	5855.086	0.0	0.0	23.6
4.61	6093.649	28.6	29.6	34.2
4.61	6639.717	19.9	23.6	24.6
4.61	6705.105	45.3	44.5	46.2
4.61	6726.673	49.0	47.8	49.3
4.61	6810.267	44.7	54.5	0.0
4.61	6841.341	61.7	67.2	65.5
4.61	6858.155	51.0	51.9	56.8
4.64	6733.153	23.9	28.1	30.8
4.64	6752.716	35.4	35.6	39.9
4.64	6820.374	40.6	43.2	40.3
4.64	6828.596	57.3	55.5	55.1
4.64	6842.689	35.7	37.7	40.1
4.65	5679.032	60.8	61.3	59.6
4.65	5927.797	41.7	43.9	32.5
4.65	5930.191	84.2	86.2	79.7
4.65	6007.968	59.5	59.2	62.2
4.65	6079.016	45.1	46.1	43.4
4.65	6804.010	18.3	24.7	22.6
4.73	5984.826	82.6	85.2	76.9

TABLE 1. CONTINUED

χ_{ℓ}	λ	$W_{\lambda}(\mu=1.0)$	$W_{\lambda}(\mu=0.5)$	$W_{\lambda}(\mu=0.3)$
4.73	6056.013	72.4	71.6	69.7
4.73	6290.974	72.8	71.2	70.5
4.73	6330.852	34.0	34.1	34.8
4.73	6419.956	88.9	91.1	81.5
4.79	5987.070	75.1	76.3	79.3
4.79	6078.766	74.2	73.7	71.7
4.79	6338.880	43.6	47.4	47.0
4.79	6364.369	27.6	30.8	30.2
4.79	6496.472	62.3	63.2	60.4
4.79	6634.123	29.1	36.4	37.0
4.79	6713.745	17.3	22.6	22.4
4.83	5975.353	45.0	49.2	49.8
4.83	6102.183	75.4	75.2	73.2
4.83	6633.427	23.5	27.4	27.4
4.99	5633.953	64.2	67.1	63.2
5.01	6245.891	2.7	0.0	3.0
5.02	6089.574	31.6	35.9	35.1
5.03	5655.500	78.4	60.2	66.5
5.06	5655.183	60.0	47.4	49.5
5.08	5650.694	37.2	38.5	37.5

Table 2. IRON ABUNDANCES DETERMINED FROM MUTSCHLECNER'S MODEL

$\bar{\chi}_\ell$	μ = 1.0 log A	μ = 1.0 No. Lines	μ = 0.5 log A	μ = 0.5 No. Lines	μ = 0.3 Log A	μ = 0.3 No. Lines
1.0	-5.08	(11)	-5.00	(11)	-4.98	(11)
2.25	-5.25	(29)	-5.21	(30)	-5.16	(31)
2.75	-5.26	(20)	-5.23	(21)	-5.17	(20)
3.25	-5.32	(7)	-5.32	(6)	-5.24	(6)
3.75	-5.43	(25)	-5.42	(26)	-5.36	(25)
4.25	-5.37	(44)	-5.37	(44)	-5.33	(47)
4.75	-5.18	(56)	-5.14	(55)	-5.13	(56)
5.05	-4.95	(5)	-5.02	(5)	-4.95	(4)

log A = log N_{Fe}/N_H

Table 3. VALUES OF $\Delta\theta$ DETERMINED FOR DIFFERENT PHOTOSPHERIC MODELS

Model	μ=1.0	μ=0.5	μ=0.3
Elste's Model 10 Isotropic Turbulence	0.07	0.08	0.08
Elste's Model 10 Holweger's Turbulence	0.08	0.08	0.08
Holweger	0.10	0.11	0.11
Mutschlecner	0.09	0.10	0.10
Utrecht Reference Model	0.05	0.06	0.08
Three Stream Model	0.07	0.08	0.08

Table 4. IRON ABUNDANCES LOG N_{Fe}/N_H DETERMINED FOR DIFFERENT PHOTOSPHERIC MODELS

Model	μ=1.0	μ=0.5	μ=0.3
Elste's Model 10 Isotropic Turbulence	-5.45	-5.42	-5.39
Elste's Model 10 Holweger's Turbulence	-5.44	-5.47	-5.45
Holweger	-5.32	-5.35	-5.33
Mutschlecner	-5.38	-5.34	-5.30
Utrecht Reference Model	-5.47	-5.52	-5.54
Three Stream Model	-5.47	-5.40	-5.33

Figure 1. A curve-of-growth for the center of the disk. The curve fitted to the points is a theoretical curve calculated for χ_{ℓ} = 3.5 volts and λ = 6000 Å.

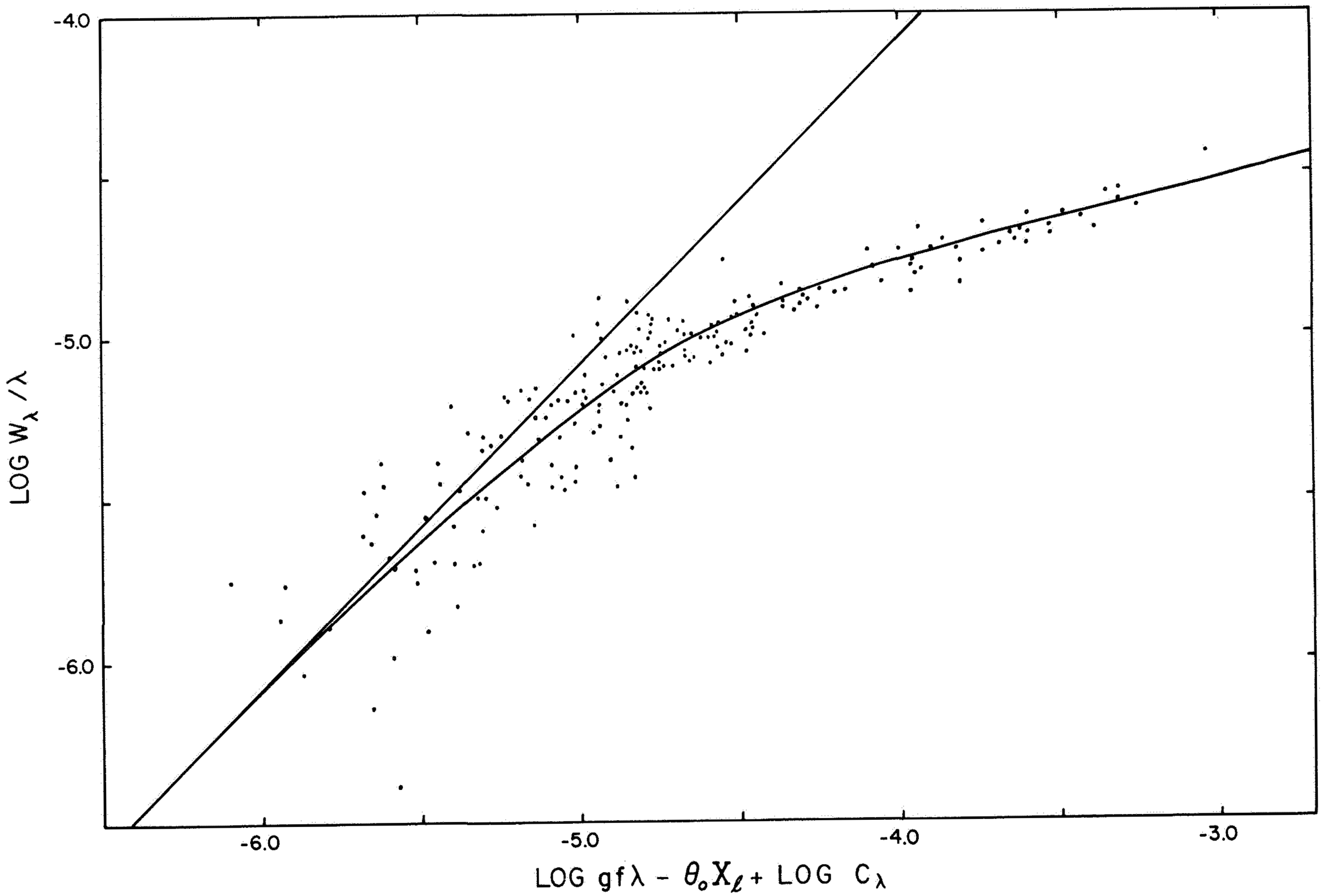
-4.0
-5.0
-6.0
LOG W_λ/λ
-6.0
-5.0
-4.0
-3.0
LOG $gf\lambda - \theta_o X_\ell$ + LOG C_λ

Figure 2. The depth dependence of the electron temperature in several photospheric models: —x— —x— Holweger; — — — Model 10; ———— Mutschlecner; —-— Utrecht Reference Model;...... cool stream for the three stream model; .•...•. hot stream for the three stream model; Model 10 is the medium temperature stream for the three stream model.

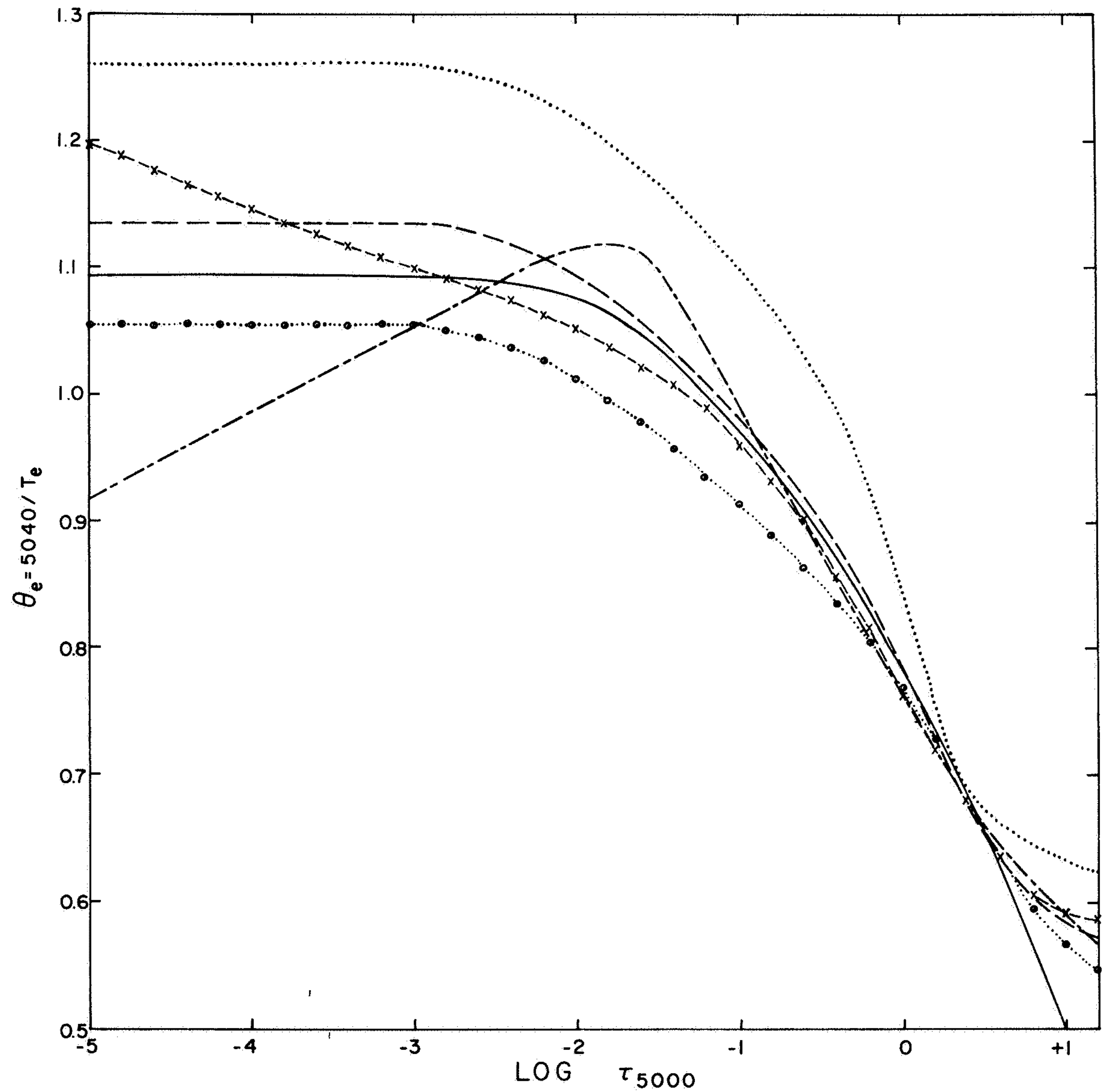

1.3
1.2
1.1
1.0
0.9
0.8
0.7
0.6
0.5
θe=5040/Te
-5
-4
-3
-2
-1
0
+1
LOG τ5000

Figure 3. The solar iron abundance, log N_{Fe}/N_H, plotted as a function of the lower excitation potential, χ_ℓ, for μ = 1.0, 0.5, and 0.3. Corliss and Warner's gf-values were used in determining the abundances.

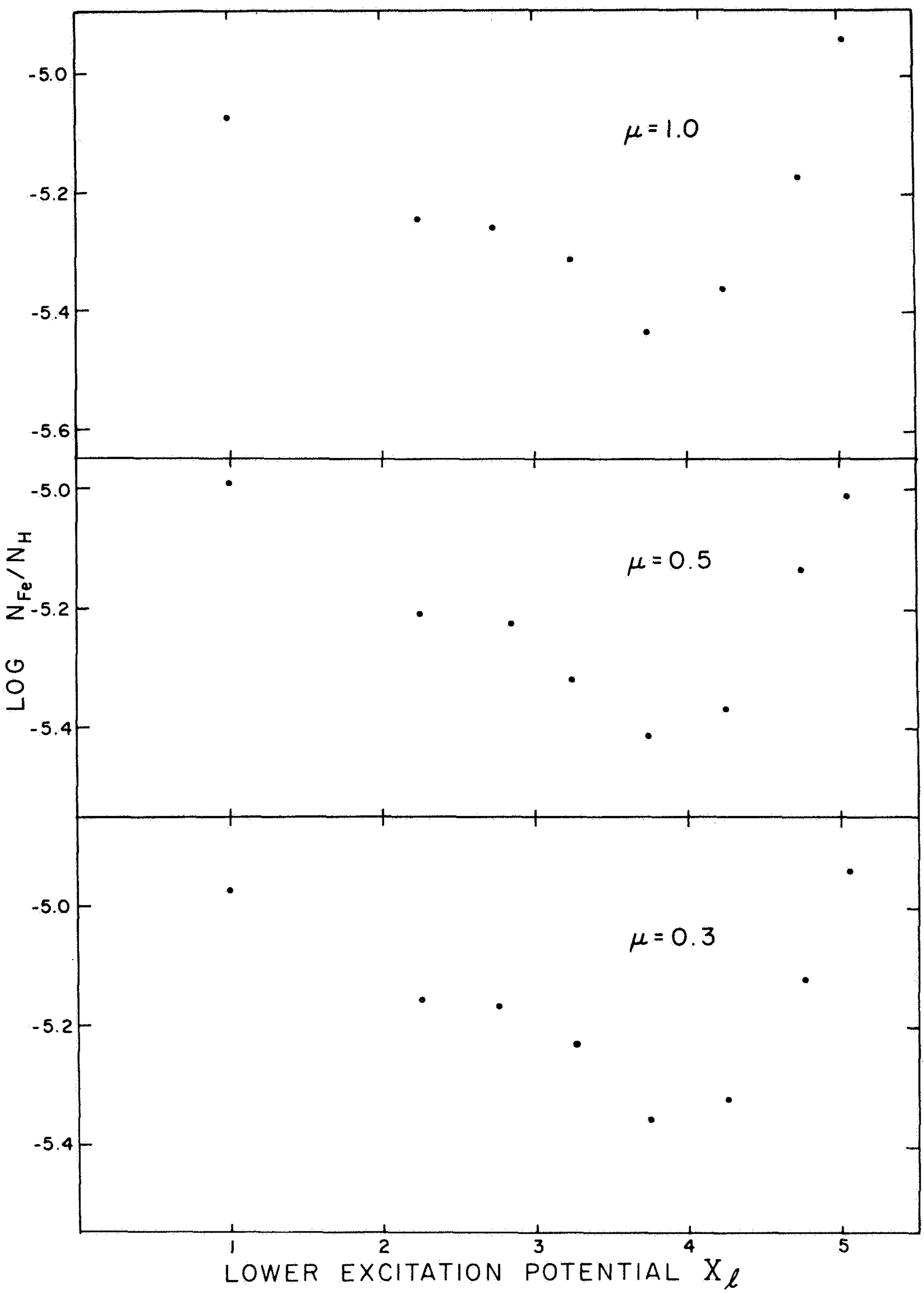

-5.0
-5.2
-5.4
-5.6
$\mu = 1.0$
-5.0
-5.2
-5.4
$\mu = 0.5$
-5.0
-5.2
-5.4
$\mu = 0.3$
LOG N_{Fe}/N_H
1
2
3
4
5
LOWER EXCITATION POTENTIAL X_ℓ

Figure 4. The solar iron abundance plotted as a function of χ_{ℓ} for μ = 1.0, 0.5, and 0.3. The corrected CW gf-values (see text) were used in determining the abundances.

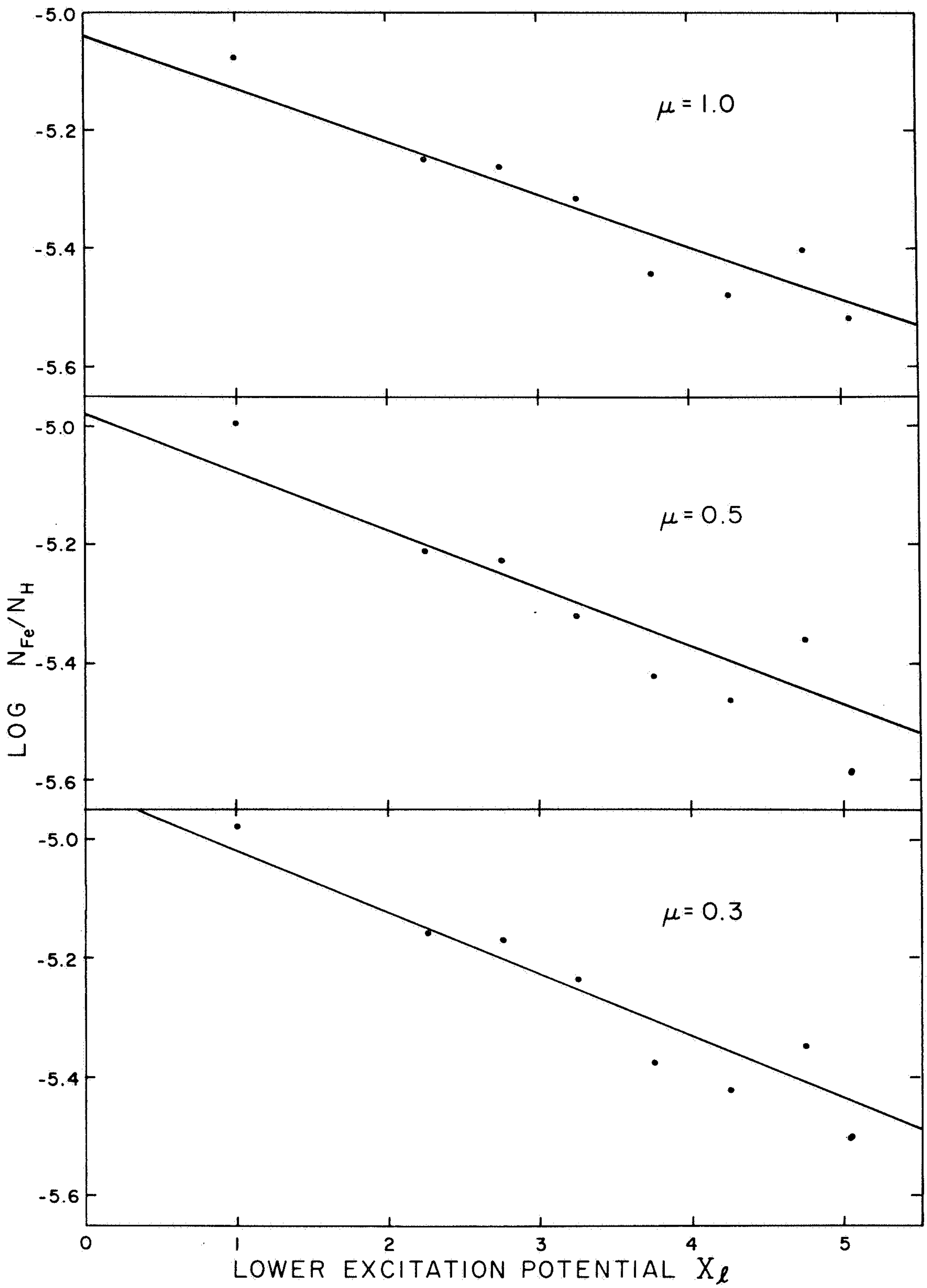

-5.0
-5.2
-5.4
-5.6
μ = 1.0
μ = 0.5
μ = 0.3
LOG N_{Fe}/N_H
0
1
2
3
4
5
LOWER EXCITATION POTENTIAL χ_ℓ

Figure 5. Solar abundances determined from individual lines plotted as a function of the upper excitation potential, χ_u. The CW gf-values were used.

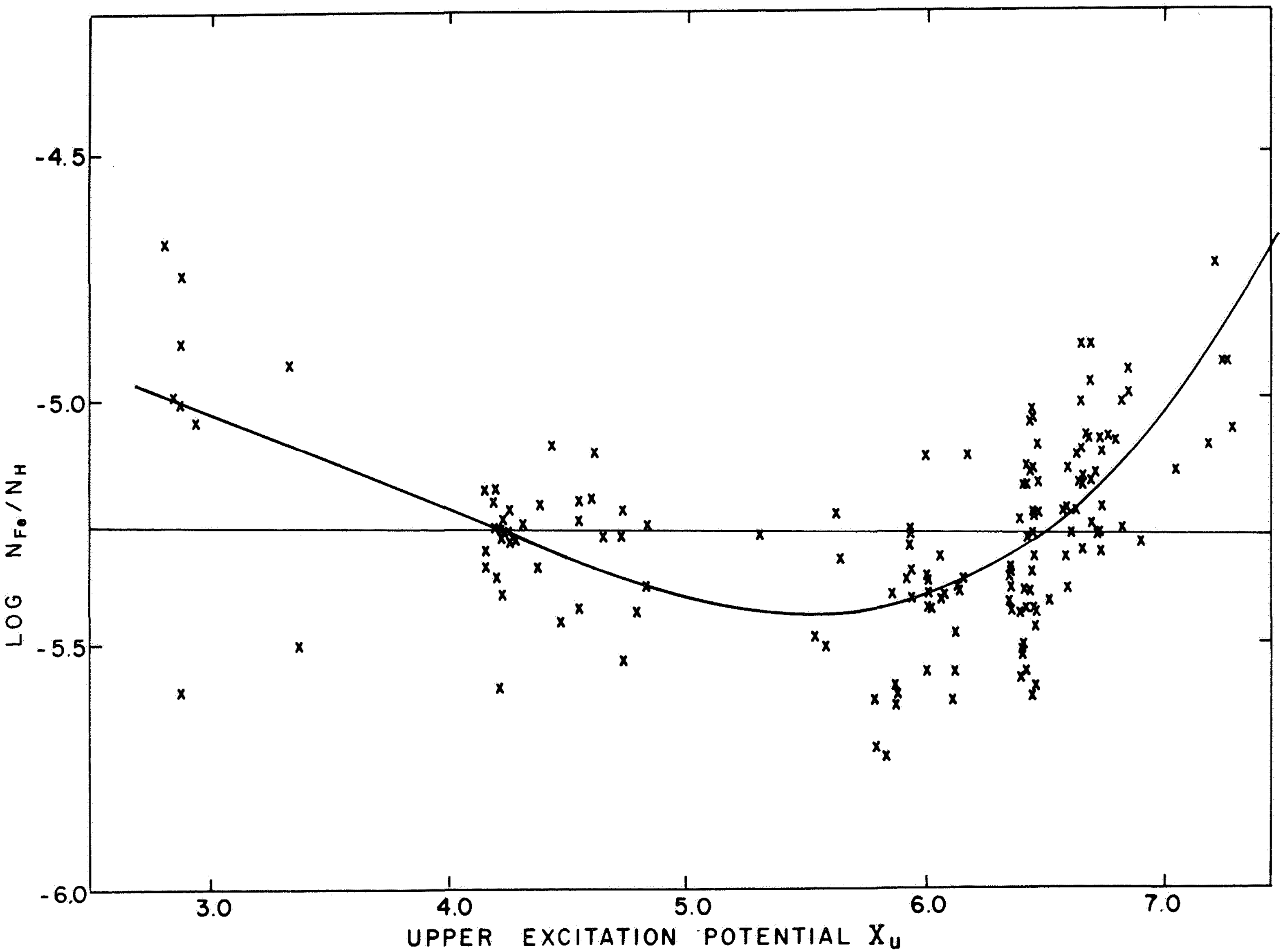

-4.5
-5.0
-5.5
-6.0
LOG N_{Fe}/N_H
3.0
4.0
5.0
6.0
7.0
UPPER EXCITATION POTENTIAL X_u

Figure 6. Solar abundances determined from individual lines plotted as a function of the upper excitation potential. The corrected CW gf-values (see text) were used.

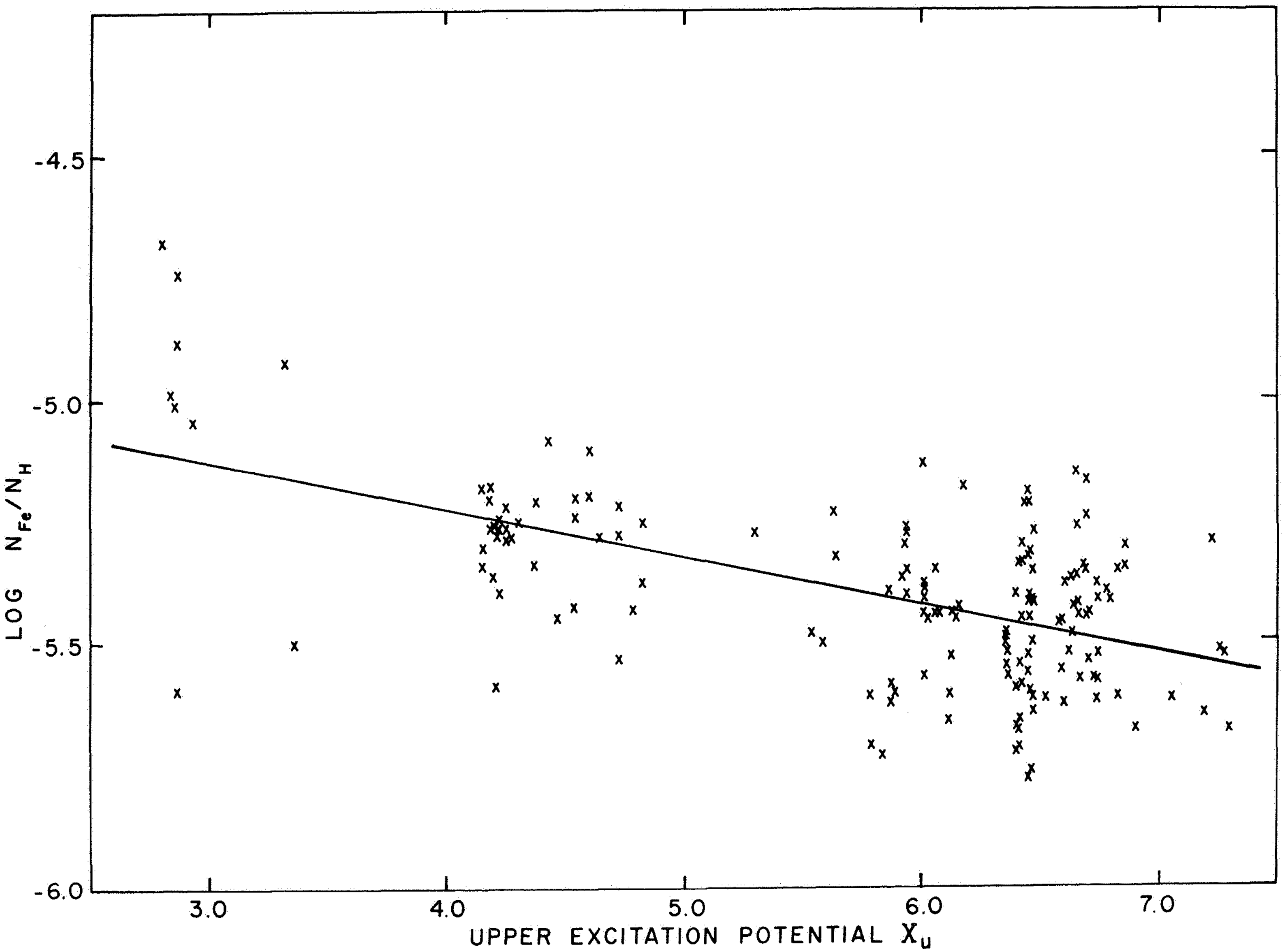
-4.5
-5.0
-5.5
-6.0
LOG N_Fe/N_H
3.0
4.0
5.0
6.0
7.0
UPPER EXCITATION POTENTIAL X_u

Figure 7. The depth-dependence of the photospheric electron temperature from Model 10 (solid line) and the excitation temperature (dashed line) used to remove the χ-dependence in the solar iron abundance.

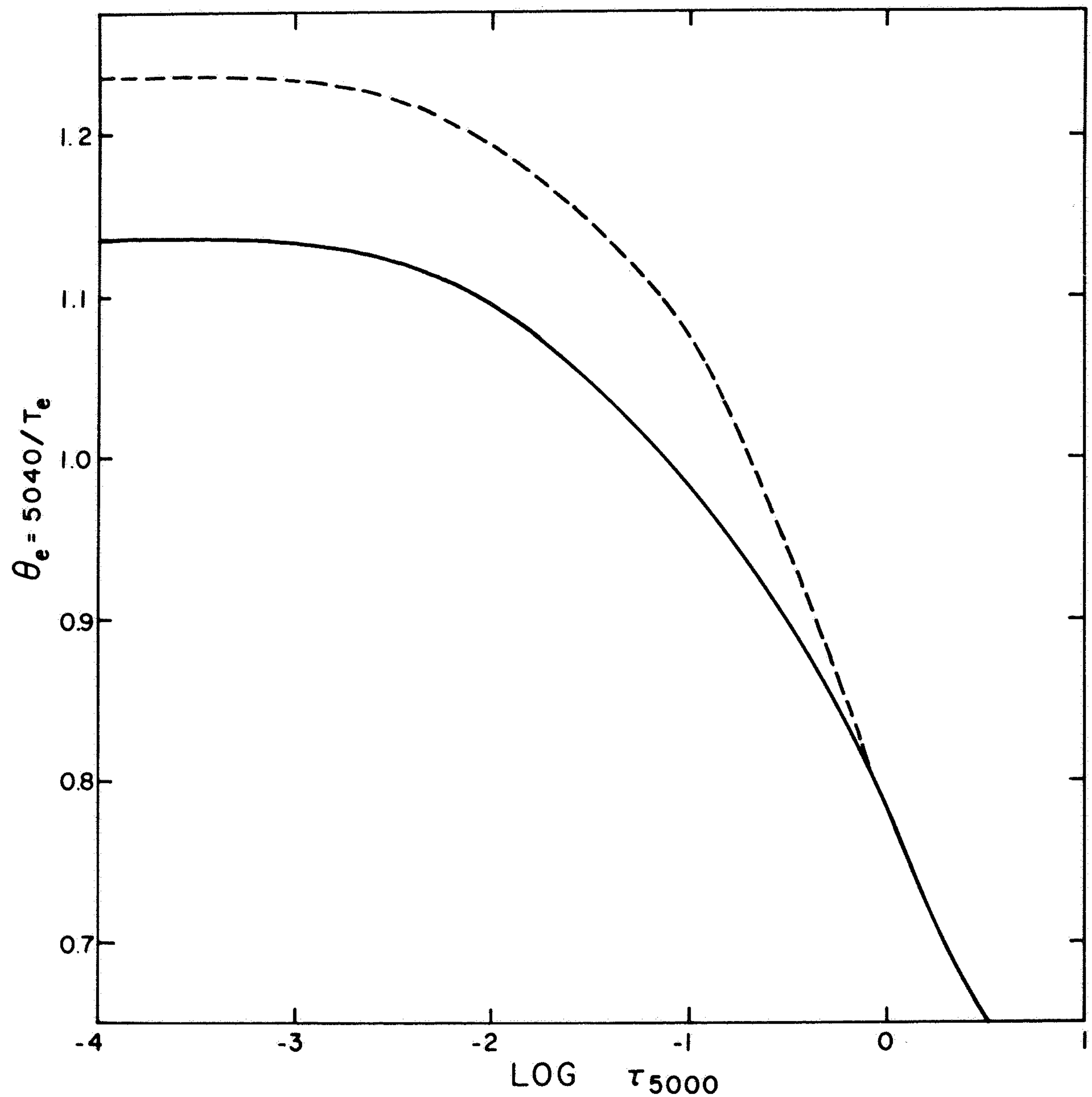

1.2
1.1
1.0
0.9
0.8
0.7
-4
-3
-2
-1
0
1
θe = 5040/Te
LOG τ5000